Published in final edited form as:
J Am Chem Soc. 2009 November 18; 131(45): 16555–16567. doi:10.1021/ja907184g.

New Strategies for the Design of Folded Peptoids Revealed by a Survey of Noncovalent Interactions in Model Systems

Benjamin C. Gorske, **Joseph R. Stringer**, **Brent L. Bastian**, **Sarah A. Fowler**, and **Helen E. Blackwell**[*]
Department of Chemistry, University of Wisconsin–Madison, 1101 University Avenue, Madison, WI 53706-1322

Abstract

Controlling the equilibria between backbone *cis*- and *trans*-amides in peptoids, or *N*-substituted glycine oligomers, constitutes a significant challenge in the construction of discretely folded peptoid structures. Through the analysis of a set of monomeric peptoid model systems, we have developed new and general strategies for controlling peptoid conformation that utilize local noncovalent interactions to regulate backbone amide rotameric equilibria, including n→π*, steric, and hydrogen bonding interactions. The chemical functionalities required to implement these strategies are typically confined to the peptoid side chains, preserve chirality at the side chain *N*-α-carbon known to engender peptoid structure, and are fully compatible with standard peptoid synthesis techniques. Our examinations of peptoid model systems have also elucidated how solvents affect various side chain-backbone interactions, revealing fundamental aspects of these noncovalent interactions in peptoids that were largely uncharacterized previously. As validation of our monomeric model systems, we extended the scope of this study to include peptoid oligomers and have now demonstrated the importance of local steric and n→π* interactions in dictating the structures of larger, folded peptoids. This new, modular design strategy has guided the construction of peptoids containing 1-naphthylethyl side chains, which we show can be utilized to effectively eliminate *trans*-amide rotamers from the peptoid backbone, yielding the most conformationally homogeneous class of peptoid structures yet reported in terms of amide rotamerism. Overall, this research has afforded a valuable and expansive set of design tools for the construction of both discretely folded peptoids and structurally-biased peptoid libraries, and should shape our understanding of peptoid folding.

Introduction

The family of oligomers comprising poly-*N*-substituted glycines, or “peptoids”, was originally conceived to address the early demands of combinatorial chemistry for efficient library synthesis.[1, 2] This legacy is manifest in the peptoid submonomer synthesis method, which is capable of delivering sizable and structurally diverse peptoid libraries derived from a continually expanding pool of commercially available primary amines.[3] As such, thousands of peptoid monomers are now readily accessible via this protocol, rivaling if not exceeding the number of amino acids available for the construction of analogous peptide libraries. Resistance to proteolysis[4] and rapid cellular uptake[5] have further rendered peptoids attractive candidates for biological applications. Screening of peptoid libraries, both random and focused, has yielded numerous bioactive compounds, including antimicrobial agents,[6]

[*]Corresponding author. Phone: 608/262-1503; Fax: 608/265-4534, blackwell@chem.wisc.edu.

Supporting Information Available: Full characterization data for model peptoids, HPLC data for peptoid pentamers, NMR spectra for model systems and pentamers, computational data, and a complete author list for the reference in footnote 1. This material is available free of charge via the Internet at http://pubs.acs.org.

neutralizers of bacterial endotoxins,[7] lung surfactants,[8] drug delivery vehicles,[9] and ligands for pharmaceutically relevant targets such as the HDM2 protein,[10] G-protein-coupled receptors,[11] and the SH3 domains of signaling proteins.[12] Apart from biological applications, screening of peptoids has also produced new DNA drag tags,[13] chemical sensors,[14] and organocatalysts.[15, 16]

The decoration of discretely folded oligomeric scaffolds with chemical functionality in a combinatorial fashion has proven an attractive strategy for library focusing.[17–19] The design of such libraries requires a thorough understanding of the folding propensities of the chosen oligomeric scaffolds. This view, in part, has motivated enormous efforts to decipher the relationships between sequence and secondary structure in biopolymers such as peptides and proteins. These relationships have already been used to efficiently bias peptide libraries[20] and have also greatly benefited the understanding of synthetic foldamers, but compared to peptides and proteins, the folding of peptoids has not been as extensively studied. Indeed, considering the tremendous potential demonstrated by peptoids in the short time since their inception, the intramolecular interactions that direct their folding remain largely unclear, even in comparison to other foldamer systems such as β-peptides.[21] A deeper understanding of the peptoid folding process would certainly contribute to the rational design of peptoid structures competent for a wide range of applications, and likely increase the utility of future peptoid libraries.

Early research on peptoid secondary structure revealed the propensity of peptoids to adopt helical structures analogous to the *cis*-amide polyproline I (PPI) helix.[22–24] *N*-α-chiral side chains were shown to promote the folding of these structures in both solution[25] and the solid state,[26] despite the lack of main chain chirality and secondary amide hydrogen bond donors crucial to the formation of many α-peptide secondary structures (Figure 1). Although computational studies initially suggested that steric interactions between *N*-α-chiral aromatic side chains and the peptoid backbone primarily dictated helix formation,[27] both intra- and intermolecular aromatic stacking interactions have also been proposed to participate in stabilizing such helices.[23, 25, 27] Other classes of peptoid side chains have been designed to introduce dipole-dipole, hydrogen bonding, and electrostatic interactions that stabilize the peptoid helix, although their development typically has not encompassed scrutinizing the individual noncovalent interactions involved.[24, 28–30] The majority of these strategies rely on incorporation of *N*-α-chiral centers in order to impart helix handedness. However, a facile equilibration between the *cis*- and *trans*-conformations of the tertiary backbone amides often counters these organizing influences by giving rise to significant populations of both rotamers, leading to disruption and fraying of peptoid helices, especially at the termini.[25] The inherent flexibility of peptoids in general can lead to coexisting and potentially inter-converting conformers in solution, making analysis of peptoid structure less than straightforward.[25] Moreover, this conformational heterogeneity complicates the *de novo* design of new peptoid secondary structures.

A recent report describing a distinctive threaded loop secondary structure adopted by several peptoid homononamers composed of *N*-α-chiral amide side chains has provided new insights into how peptoid amide isomerization might be controlled.[31] Notably, this loop structure contains both *cis*- and *trans*-amides, and is stabilized by hydrogen bonds between the peptoid backbone and the *N*-terminal ammonium group. These hydrogen bonds are apparently of sufficient strength as to overwhelm the helical propensities resulting from local interactions between the side chains and the backbone. This finding — that a relatively small number of noncovalent interactions can stabilize both *cis*- and *trans*-amides within the backbones of large peptoid structures — suggests that strategically positioned noncovalent interactions could be harnessed to rationally control amide isomerism and generate new peptoid structural motifs. In this context, peptoids stand apart from typical peptides and

other secondary amide-based foldamers in that their tertiary amide backbones are devoid of hydrogen bond donors, creating a unique opportunity to rationally control the distribution of these donors by selection of appropriate hydrogen bonding side chains. Such engineered hydrogen bonding networks could conceivably act as templates for both inter- and intramolecular structural assembly. Alternatively, the elimination of hydrogen bonding motifs in peptoids would greatly facilitate investigations of other more subtle noncovalent interactions that, while relatively weak individually, might collectively exert significant influences on peptoid structure.

We have undertaken a research program focused on characterizing the roles of hydrogen bonding and other noncovalent interactions in directing peptoid amide isomerism, and thereby, peptoid folding in general. The recent focus of these studies has been on small, peptoid model systems. The principal objective of these studies was to isolate and characterize only the local interactions between peptoid side chains and the backbone, in the hope that this restriction might yield highly modular and easily applicable design criteria for controlling the structures of larger peptoid oligomers. We recently reported the initial findings of these studies, which showed that n→π* interactions can regulate peptoid amide isomerism in monomeric peptoid model systems.[32, 33] However, the roles that these interactions might play in determining the folded structures of actual oligomeric peptoids remained unexplored. Here, we present a comprehensive overview of our investigations in this area to date that encompass a much wider range of side chain structures, noncovalent interaction classes, and solvents. We have developed several new and general strategies for controlling peptoid conformation that utilize local noncovalent interactions to regulate backbone amide isomerism. The chemical functionalities required to implement these strategies typically are confined to the peptoid side chains, preserve the chirality of the side chain at the *N*-α-carbon, and are fully compatible with standard peptoid synthesis techniques. Our examinations of peptoid model systems have also elucidated how various side chain-backbone interactions are affected by solvent, revealing fundamental aspects of these noncovalent interactions in peptoids that were largely uncharacterized previously in the literature. As validation of these monomeric model systems, we extended the scope of the study to include longer peptoid oligomers that demonstrate the importance of such noncovalent interactions within the context of larger, structured peptoids. This modular approach to peptoid design culminated in the installation of 1-napthylethyl side chains into a series of peptoid oligomers, which were found to virtually suppress *trans*-amide rotamers in the backbone and consequently should prove to be valuable structure-promoting elements in peptoids. Indeed, our preliminary structural characterization suggests that these oligomers represent the most conformationally defined, acyclic *cis*-peptoids yet reported. Collectively, this work has afforded a valuable new set of approaches for the rational design of both folded peptoids and structurally biased peptoid libraries, and should contribute to the growing understanding of peptoid folding.

Experimental Section

General

All reagents were purchased from commercial sources (Alfa-Aesar, Aldrich, Advanced ChemTech, and Acros) and used without further purification. Solvents were purchased from commercial sources (Aldrich and J. T. Baker) and used as is, with the exception of dichloromethane (CH_2Cl_2) and *n*-hexane, which were distilled immediately prior to use. Thin layer chromatography (TLC) was performed on silica gel 60 F_{254} plates (E-5715-7, EMD). SiliaFlash® P60 silica gel (40–63 μm, Silicycle) was used for manual flash column chromatography.[34] High-pressure flash chromatography (HPFC) was performed using prepacked silica gel columns (KP-SIL, Biotage) on a Biotage SP system.

^{1}H NMR (500 MHz), ^{13}C NMR (125 MHz), and ^{19}F NMR (470 MHz) spectra were recorded on either a Varian Unity or an Inova 500 MHz spectrometer in deuterated solvents. ^{1}H NMR (300 MHz), ^{13}C NMR (75 MHz), and ^{19}F NMR (282 MHz) spectra were recorded on either a Bruker AC-300 or a Varian MercuryPlus 300 spectrometer in deuterated solvents. Chemical shifts are reported in parts per million (ppm, δ) using tetramethyl silane (TMS) as a reference (0.0 ppm), unless otherwise noted. Couplings are reported in hertz. Nuclear Overhauser effect spectroscopy (NOESY), gradient double quantum filtered correlation spectroscopy (gDQCOSY), and heteronuclear single quantum coherence adiabatic (HSQCAD) NMR experiments were performed on a Varian Inova 500 or 600 MHz spectrometer, and were referenced to solvent. The data were processed using the Varian VNMR software package (v. 6.1C) and visualized using SPARKY software.[35]

Electrospray ionization (ESI) mass spectra were obtained on a Waters (Micromass) LCT™ spectrometer equipped with a time-of-flight analyzer. Samples were dissolved in methanol and sprayed with a sample cone voltage of 20. Electron impact (EI) mass spectra were obtained on a Waters (Micromass) AutoSpec™ spectrometer equipped with a magnetic sector. The samples were placed in a glass capillary and inserted directly into the source, and the resulting vapor was bombarded with 70 eV electrons. Perfluorokerosene (PFK) was used for calibration. Matrix-assisted laser desorption/ionization time-of-flight (MALDI-TOF) mass spectra were obtained on a Bruker REFLEX II spectrometer equipped with a 337 nm laser and a reflectron. In positive ion mode, the acceleration voltage was 25 kV.

Reversed-phase high performance liquid chromatography (RP-HPLC) was performed using a Shimadzu system equipped with an SCL-10Avp controller, a LC-10AT pump, an FCV-10ALvp solvent mixer, and an SPD-10MAvp UV/vis diode array detector. A Restek Premier C18 column (5 μm, 4.6 mm × 250 mm) was used for all analytical RP-HPLC work. A Vydac protein & peptide C18 column (10 μm, 22 mm × 250 mm) was used for all preparative RP-HPLC work. Standard RP-HPLC conditions were as follows: flow rates were 1 mL/min for analytical separations and 9 mL/min for preparative separations; mobile phase A = 0.1% trifluoroacetic acid (TFA) in water; mobile phase B = 0.1% TFA in acetonitrile. Purities were determined by integration of peaks with UV detection at 220 nm.

LC-MS data were obtained using a Shimadzu LCMS-2010 equipped with two LC-10ADvp pumps, an SCL-10Avp controller, an SIL-10ADvp autoinjector, an SPD-M10Avp UV/vis diode array detector, and a single quadrupole analyzer (for ESI). A Supelco 15 cm × 2.1 mm C18 wide-pore column was used for all LC-MS work. Standard RP-HPLC conditions for LC-MS were as follows: flow rate = 200 μL/min; mobile phase A = 0.4% formic acid in water; mobile phase B = 0.2% formic acid in acetonitrile.

Attenuated total reflectance (ATR)-IR spectra were recorded with either a Bruker Tensor 27 spectrometer outfitted with a single reflection MIRacle Horizontal ATR by Pike Technologies and a ZnSe crystal with a spectral range of 20,000 to 650 cm^{-1}, or a Bruker Equinox 55 spectrometer outfitted with a single reflection MIRacle Horizontal ATR and a Ge crystal with a spectral range of 5500 to 600 cm^{-1}. Circular dichroism (CD) spectra were obtained on an Aviv 62A DS spectropolarimeter with Aviv CDS software.

Synthesis and characterization of peptoid model systems 1–32

All peptoid model systems were synthesized in solution according to previously reported procedures.[32] Peptoid model systems **1**–**15** and **30** have been characterized previously.[32] Full characterization data for peptoid model systems **16**–**29**, **31**, and **32** are provided in the Supporting Information.

Synthesis and characterization of peptoid oligomers 33–38

Peptoids **33**–**38** were synthesized using microwave-assisted solid-phase methods on Rink-amide-derivatized polystyrene resin as previously reported.[36, 37] The crude peptoids were purified by preparative RP-HPLC and characterized by MS to confirm their identity (see Table 1). See Supporting Information for HPLC data for peptoids **33**–**38**.

Determination of *cis*/*trans* rotamer ratios ($K_{cis/trans}$) for the peptoid model systems

Each model peptoid was dissolved in the desired solvent to give a 15 mM solution. ^{1}H NMR spectra were acquired using 16 scans and a relaxation delay of 25 s. 1D-NOESY spectra were acquired to verify previously reported guidelines for distinguishing *cis*- and *trans*-amide rotamers.[31, 33] In cases where these guidelines appeared to be inapplicable, additional 1D-NOESY spectra were acquired to distinguish *cis*- and *trans*-amide rotamers. *Cis/trans* ratios were calculated by averaging the integration ratios for at least two sets of rotamer-related peaks. The *cis/trans* ratios of the hydrophobic model peptoid **4** were statistically identical at 1, 5, 15, 60, and 180 mM concentrations in the polar solvent CD_3CN, and the *cis/trans* ratios of the more hydrophilic model peptoid **27** at 1, 5, 10, 15, 25, 50, and 75 mM were statistically identical in the nonpolar solvent $CDCl_3$, suggesting that solvophobic aggregation is insignificant under the conditions examined in this study.

NMR analyses for peptoid model systems 27 and 30

Peptoids **27** and **30** were dissolved in CD_3CN to give 15 mM solutions and analyzed by NOESY as detailed below. The experiments were performed on a Varian Inova 600 MHz spectrometer using a 5 mm hcn probe.

NOESY experiments on **27** in CD_3CN were performed at 24 °C using the following parameter values: mix time = 700 ms; spectral width = 8000 Hz; number of transients (nt) = 16; number of increments (ni) = 64. The number of points (np) was 2048, and 192 points were obtained by linear prediction in the f1 dimension. Square cosine window functions were applied in both dimensions. The spectra were zero-filled to generate f1 × f2 matrices of 4096 × 4096 points. Parameters for NOESY experiments on **30** in CD_3CN were reported previously. [32]

NMR analyses for peptoid oligomers 33–38

Peptoids **33**–**38** were dissolved in CD_3CN to give 15 mM solutions and analyzed by gDQCOSY and HSQCAD NMR experiments as detailed below. The experiments were performed on a Varian Inova 600 MHz spectrometer using a 5 mm hcn probe. The gDQCOSY spectra were used for assignment purposes, and the HSQCAD NMR spectra were subsequently integrated to give the $K_{cis/trans}$ values in Table 6. Assignments of methyne *cis* and *trans* peaks were based on previously observed trends in chemical shift,[37] and verified by NOESY NMR, unless otherwise noted.

gDQCOSY NMR experiments were performed for peptoids **33**–**36** at 24 °C using the following parameter values: Spectral widths were 5323, 5287, 4727, and 6611 Hz, respectively. The numbers of transients (nt) were 8, 16, 16, and 16, respectively. The relaxation delays (d1) were 1.20, 1.12, 1.68, and 2.30, respectively. The numbers of increments (ni) were 300, 300, 300, and 256, respectively. The number of points (np) was 4096, with 1200 points obtained by linear prediction in the f1 dimension. Square cosine window functions were applied in both dimensions. The spectra were zero-filled to generate f1 × f2 matrices of 8192 × 8192 points.

HSQCAD NMR experiments[38] were performed for peptoids **33**–**38** at 24 °C using the following parameter values: Spectral widths were 5323, 5212, 4727, 6611, 5914, and 5914

Hz, respectively, in the ^{1}H dimension. Spectral widths were 28787, 28684, 30234, 36199, 30948, and 25983 Hz, respectively, in the ^{13}C dimension. The relaxation delays (d1) were 1.50, 0.84, 1.68, 2.30, 3.36, and 2.94, respectively. The number of transients (nt) were 8, 8, 8, 8, 2, and 2, respectively. The number of increments (ni) was 256, with 1200 points obtained by linear prediction in the f1 dimension. The number of points was 2048. Square cosine window functions were applied in both dimensions. The spectra were zero-filled to generate f1 × f2 matrices of 8192 × 2048 points.

CD analyses for peptoids 26, 37, and 38

Peptoid stock solutions were prepared by dissolving at least 2 mg of each peptoid in spectroscopic grade acetonitrile. The stock solutions then were diluted with spectroscopic grade acetonitrile to the desired concentration (~60 μM) by mass using a high-precision balance (Mettler-Toledo XS105). CD spectra were obtained in a square quartz cell (path length 0.1 cm) at 25 °C using a scan rate of 100 nm/min, with five averaged scans per spectrum. The spectrum of an acetonitrile blank was subtracted from the raw CD data, and the resulting data were plotted using Kaleidagraph software (v. 4.03).

Results and Discussion

Design and synthesis of peptoid model systems

We designed monomeric peptoid model systems that mimicked the local environments of isolated amide side chains within a peptoid oligomer in order to dissect short-range (*i*· · ·*i* or *i*· · ·*i*±1) interactions. Since we were primarily interested in elucidating the impact of side chain structure on backbone amide isomerism, our initial monomeric models consisted of two tertiary amides positioned opposite the side chain, as in a typical peptoid backbone. We developed two straightforward syntheses of these diamide models (Scheme 1) that were easily adapted for the installation of other *C*-terminal and *N*-terminal capping groups besides amides, such as esters.[32] This flexibility of design permitted us to probe the role of either terminus in any side chain-backbone interaction of interest in our model system.

The peptoid model system side chains and terminal capping groups examined in this study are shown in Table 2. *N*-α-chiral amide side chains are heavily represented, as these have been extensively investigated previously and found to promote peptoid helix and loop folding (see above). In addition to this consideration, side chain functionalities were selected to explore the effects of four key types of noncovalent interactions on peptoid amide *cis*/*trans* equilibria: (1) n→π* interactions between an amide and an aromatic ring (n→π^*_{Ar}), (2) n→π* interactions between two carbonyls (n→$\pi^*_{C=O}$), (3) side chain-backbone steric interactions, and (4) side chain-backbone hydrogen bonding interactions. Our analyses of each type of interaction in a series of model systems are described sequentially below. The *cis*/*trans* ratio of the *N*-terminal amide in each model system was determined by ^{1}H NMR and NOESY and used to assess the influence of the noncovalent interactions on peptoid amide isomerism.

Investigations of the impact of n→π^*_{Ar} interactions on peptoid amide rotamer equilibria

In earlier work, we observed that the incorporation of electron-deficient aromatic rings into peptoids could have a profound impact on their structure.[37,39] Analysis of related, small model systems suggested that these structural perturbations arise in part from an interaction between a lone pair of the proximal amide oxygen and a π* orbital of the electron-deficient aromatic ring, that is, an n→π^*_{Ar} interaction (also referred to as an lp-π interaction).[40, 41] This type of interaction has been loosely defined by a carbonyl oxygen-to-ring centroid distance between 2.8 and 3.8 Å, and a dihedral angle between the aryl plane and the carbonyl plane ($X_2C=O$) of 90° or less.[42] We reasoned that an interaction between an *N*-α-

chiral aromatic peptoid side chain and the nearest backbone carbonyl would easily meet these geometrical constraints and, if operative, would exclusively stabilize the *cis*-rotamer of the participating amide, increasing $K_{cis/trans}$ (Figure 2). We tested this possibility by constructing peptoid model systems **1**–**3** and examining them using ^{1}H NMR, initially focusing on the acetamide *cis*/*trans* ratios obtained in acetonitrile ($^{CD_3CN}K_{cis/trans}$), since this solvent has been commonly used in structural studies of peptoids (Figure 3, Table 3).[22, 23, 25, 37] Furthermore, this solvent minimizes inter-amide interactions that can also affect ^{K}*cis/trans*; these interactions and their solvent-dependence are discussed in the next section.

We hypothesized that model compounds **1** and **2** would exhibit higher *cis*/*trans* ratios than **3**, since electron-withdrawing groups on aromatic rings are known to increase the strength of $n\rightarrow\pi^*_{Ar}$ interactions.[41] In accord with our hypothesis, we observed a nearly two-fold increase in $^{CD_3CN}K_{cis/trans}$ for the compounds containing the electron-deficient benzyl side chains *fe* and *np* (**1** and **2**) compared to the control compound containing the unsubstituted benzyl side chain *pe* (**3**) (Table 3). Replacement of the aromatic ring with a cyclohexyl ring (*cy*, to yield **4**) lowered $^{CD_3CN}K_{cis/trans}$, as expected. Although these model systems validated the possibility of $n_i\rightarrow\pi_{i+1}{}^*_{Ar}$ interactions in a typical peptoid, an $n_i\rightarrow\pi_i{}^*_{Ar}$ interaction involving the *C*-terminal amide could not be excluded. We thus constructed control compounds **5**–**7**, in which the *C*-terminal amide was replaced with a methyl group (Figure 3). This series of compounds exhibited nearly identical $^{CD_3CN}K_{cis/trans}$ values to the piperidinyl series (**2**–**4**), suggesting that $n_i\rightarrow\pi_i{}^*_{Ar}$ interactions do not significantly regulate peptoid amide isomerism, and establishing that the *C*-terminal amide has little impact on $^{CD_3CN}K_{cis/trans}$ in these systems (Table 3). We also synthesized formally charged model systems (pyridinium **8** (*4mpy*) and phenolate **9** (*mph*), Figure 3) to further explore the possibility of controlling $K_{cis/trans}$ by tuning the electronics of *N*-α-chiral aromatic side chains. As expected, the presence of *mph* in **9** substantially demoted the *cis*-amide rotamer relative to *pe* in **6**, while the *4mpy* side chain in **8** strongly promoted the *cis*-amide. Comparison of NOESY NMR data for model compounds **6** and **8** indicated that the conformation in which the aromatic ring and the amide carbonyl are eclipsed is significantly more populated by **8** than by **6** (Figure 4), implying that carbonyl-aromatic interactions dictate $K_{cis/trans}$ in these systems.

Our previously reported calculations of Mulliken atomic charges suggested that electrostatic interactions between the atoms directly participating in the $n\rightarrow\pi^*_{Ar}$ interaction do not contribute considerably to $K_{cis/trans}$ in this class of peptoid model systems (**5**, **6**, **8**, and **9**).[32, 43] On the contrary, the calculations indicated that $K_{cis/trans}$ correlates closely with the LUMO energy, and even more strikingly with the LUMO density at the carbon in the aromatic ring connected to the side chain. We sought to decouple, as much as possible, the contributions of electrostatic and stereoelectronic influences on $n\rightarrow\pi^*_{Ar}$ interactions to complement these computational data. Solvent modulation is a useful approach for probing noncovalent interactions,[44–46] even though its impact on a particular interaction of interest can be somewhat obscured by solvent-charge screening and/or by perturbations elsewhere in the molecule. We thus proceeded to determine $K_{cis/trans}$ values for the structurally simplest series — the methyl-capped compounds **5**–**7** — in a range of solvents (Table 3).

$K_{cis/trans}$ for compound **7** (*ch*), which served as a baseline indicator of solvent effects on $K_{cis/trans}$ in the absence of n→π* interactions, generally tracked with solvent polarity but displayed only slight sensitivity to the choice of solvent (Table 3). The aromatic side chain of **6** (*pe*) did not significantly sensitize $K_{cis/trans}$ to solvent polarity compared to **7**, as indicated by the similar (differing by less than 0.1 kcal) differences in $\Delta G_{cis/trans}$ observed between solvents for **6** and **7**. However, **5** (*np*) diverged significantly ($\Delta G_{cis/trans}$ differing by more than 0.2 kcal) from this trend, exhibiting a *larger* $K_{cis/trans}$ in $CDCl_3$. Chloroform

would not be expected to enhance withdrawal of electron density from the aromatic ring by the nitro group (thereby lowering the aryl LUMO energy and increasing $K_{cis/trans}$), as the resulting polarization would be less stabilized by such a nonpolar solvent. Therefore, this divergence may derive from electrostatic/dipole-dipole interactions between the nitro group and the acetamide that reinforce the n→π*$_{Ar}$ interaction in $CDCl_3$. These electrostatic interactions would likely be more effectively screened in more polar solvents such as methanol; however, $^{CD_3OD}\Delta G_{cis/trans}$ for **5** remained significantly lower than for **6**, and $\Delta G_{cis/trans}$ for **5** and **6** were similarly affected by switching the solvent from acetonitrile to methanol, suggesting that electrostatic interactions are less important than the n→π*$_{Ar}$ orbital interactions in this case. Indeed, even in aqueous solution, we observed that the *cis*-amide rotamer of **8** (*4mpy*) is dominant ($^{D_2O}K_{cis/trans}$ = 3.92), demonstrating that the side chain-backbone interactions in these highly polarized systems are robust, even in strongly polar solvents that would be expected to significantly screen electrostatic interactions. This finding suggests that the inclusion of these charged aromatic monomers could produce water-soluble peptoid helices with enhanced conformational stability relative to *pe* homooligomers; such scaffolds could be valuable for biological applications. The impact of n→π*$_{Ar}$ interactions in general on the structures of peptoid oligomers is examined further in the last section of this paper.

Investigations of the impact of n→π*$_{C=O}$ interactions on peptoid amide rotamer equilibria

Having scrutinized n→π*$_{Ar}$ interactions in model systems containing a single amide, we turned our attention to diamide peptoid model systems that might more accurately reproduce the local environment experienced by a peptoid monomer unit within a larger peptoid oligomer. As discussed above, we observed that the presence of a piperidinyl amide at the *C*-terminus did not significantly perturb $^{CD_3CN}K_{cis/trans}$ for the *N*-terminal acetamide relative to the single amide models (*e.g.*, **2**–**4** vs. **5**–**7)**. Nonetheless, we were intrigued by recent literature reports by Raines, Wennemers, and co-workers of n→π*$_{C=O}$ interactions between tertiary prolyl amides and their considerable importance in stabilizing the *trans*-amides of polyproline II (PPII) helices.[47–50] Similar to the n→π*$_{Ar}$ interactions discussed above, these interactions are characterized by donation of electron density from an amide carbonyl lone pair into the π* orbital of an adjacent carbonyl. Due to geometric and stereoelectronic differences between the π* orbitals of aromatic rings and amides, a somewhat more restricted set of geometric constraints has been demarcated for n→π*$_{C=O}$ interactions ($O_{i-1}\cdots C_i{=}O_i$ distance ≤ 3.2 Å, angle = 109° ± 10°; Figure 5)[47] relative to n→π*$_{Ar}$ interactions. These constraints preclude *cis*-amides from acting as donors in *i*· · ·*i*+1 n→π*$_{C=O}$ interactions along the backbone, and n→π*$_{C=O}$ interactions are thus observed to exclusively stabilize *trans*-amide donors in polyprolines.

The strong similarity between the tertiary amide backbones of peptoids and polyprolines caused us to speculate that these n→π*$_{C=O}$ interactions could also be exploited to stabilize *trans*-amides in peptoids, providing a design strategy complementary to the *cis*-amide-stabilizing n→π*$_{Ar}$ interactions described above. Previous studies have shown that esters are excellent acceptors for these n→π*$_{C=O}$ interactions due to significantly reduced π-electron delocalization into the carbonyl π* orbital.[33, 51, 52] This reduction of electron donation into the carbonyl lowers the energy of the π* orbital, enhancing n→π*$_{C=O}$ interactions in esters relative to amides, just as removing substituents that donate electrons into aromatic rings (*e.g.*, **9** vs. **6** above) enhances n→π*$_{Ar}$ interactions. We hypothesized that amides disfavoring π-electron delocalization might also enhance n→π*$_{C=O}$ interactions, albeit to a lesser extent than esters. To test this hypothesis and probe for the presence of n→π*$_{C=O}$ interactions within peptoids in general, we constructed model systems possessing methyl esters and dimethylamides at the *C*-terminus (**10**–**15**, Figure 3). As noted in the previous section, piperidinyl amide-capped compounds **2**–**4** did not exhibit any evidence of these

interactions in acetonitrile, giving nearly identical $^{CD_3CN}K_{cis/trans}$ values to those of the methyl-capped compounds **5**–**7**. However, we expected that the dimethylamide would be somewhat less capable of stabilizing positive charge at the nitrogen compared to the piperidinyl amide, and thus might participate in an n→π*$_{C=O}$ interaction with the *N*-terminal acetamide. Analogous to the studies above, we also examined these systems in a range of solvents (Table 3).

We were pleased to observe that the nature of the *C*-terminal cap dramatically modulated the acetamide *cis-trans* equilibrium, with the ester group (in **10**–**12**) producing the largest reductions in $K_{cis/trans}$ relative to the methyl- and piperidinyl-amide-capped systems (**2**–**4**), as predicted. Although stabilization of the *trans*-amide in the dimethylamide systems (**13**–**15**) relative to compounds **2**–**4** was modest, the former demonstrated the feasibility of inter-amide n→π*$_{C=O}$ interactions within larger peptoid oligomers. We were especially intrigued by the large increases in $\Delta G_{cis/trans}$ observed upon decreasing the solvent polarity for the piperidinyl and dimethyl amide series, relative to the ester series. Since previous studies have shown that n→π*$_{C=O}$ interactions are primarily hyperconjugative rather than electrostatic in nature,[53, 54] we hypothesized that the greater solvent sensitivity of $\Delta G_{cis/trans}$ for the amides (**2**–**4**, **13**–**15**) versus the esters (**10**–**12**) may be due to reduced charge separation within the more polarizable piperidinyl and dimethylamides in nonpolar solvents. Such suppression of amide resonance would be expected to increase the strength of n→π*$_{C=O}$ interactions by lowering the energy of the π* orbital.[33] Although some debate over the significance of amide resonance has emerged,[55, 56] the greater polarizability of amides, defined here as their capacity to accommodate internal charge separation via resonance, is commonly cited to explain their significantly higher rotational barriers (~18 kcal/mol) compared to esters (~10 kcal/mol) and carbamates (~15 kcal/mol),[57–60] Indeed, the greater sensitivity of amide rotational barriers to solvent polarity, compared to that of carbamates, has been attributed to the less polarizable “ester-type resonance” in the latter.[59] In the context of this argument, the absence of n→π*$_{C=O}$ interactions for compounds **2**–**4** in acetonitrile can be ascribed to the high degree of amide polarization facilitated by the both the piperidinyl substituent and the polar solvent.

Interestingly, the amide-capped systems (**2**–**4**, **13**–**15**) showed a marked *increase* in $\Delta G_{cis/trans}$ in methanol as compared to acetonitrile, deviating from the solvent polarity trend above, while $\Delta G_{cis/trans}$ for the methyl- and ester-capped systems (**5**–**7**, **10**–**12**) remained relatively constant in both solvents. This implies that amide-amide n→π*$_{C=O}$ interactions, but not amide-ester interactions or isolated amide rotameric equilibria, are strongly affected by solute-solvent hydrogen bonding in these systems. Since esters are known to be poorer hydrogen bond acceptors than amides,[61] these data suggest that hydrogen bonds to the amide acceptors of n→π*$_{C=O}$ interactions may enhance these interactions. Further corroboration of these hypotheses in the context of peptoids containing amide and ester side chains is described later in this paper.

Investigations of the impact of steric interactions on peptoid amide rotamer equilibria

Steric interactions play an extremely important role in peptoid folding by constraining the rotations of bonds within the peptoid backbone. For example, it is these interactions that likely transmit chirality from the *N*-α-chiral peptoid side chains to the backbone, imparting “handedness” to the peptoid helix.[27] Steric interactions in peptoids are expected to be highly robust in that they are relatively unaffected by solvation.[24] This property also greatly simplifies their computational simulation and facilitates their utilization for rational design applications, as aptly illustrated by the successful computational prediction of the peptoid helical structure.[27] Although computations predict that steric interactions restrict all three peptoid backbone torsions (φ, ψ, and ω),[27] the present study focuses on the roles of these interactions in regulating peptoid amide isomerism (ω) by systematically probing the steric

profiles of peptoid side chains in a series of model systems typically containing a *C*-terminal piperidinyl amide (**16**–**26**; Figure 6, Table 4).

In general, increasing the steric bulk of the peptoid side chain in the model systems should increase the population of the *cis*-amide isomer, since the relatively small carbonyl oxygen, as compared to the acetamide methyl group, can more easily accommodate steric crowding.[27] Comparison of the $\Delta G_{cis/trans}$ values within each solvent demonstrates that these systems largely conform to this paradigm. The solvent-dependent trends observed largely mirror those of piperidinyl amides **1**–**4** (Table 3) and are consistent with the action of n→π* interactions, as discussed in the previous sections. The sole exception is compound **23**, which lacks a *C*-terminal carbonyl and exhibits little solvent-dependent change in $K_{cis/trans}$, as expected. We observed that complete removal of all *N*-α-substituents (*i.e.*, *Me*, **16**) produced a very low average $K_{cis/trans}$ value for the solvents examined ($^{AVG}K_{cis/trans}$), in keeping with this steric argument (Table 4) and in agreement with previous studies of similar *N*,*N*-dialkyl amides.[62] Although a single appended methyl group (*Et*, **17**) gave a similarly low value for $^{AVG}K_{cis/trans}$, further substitution at the *N*-α-carbon (*ip*, **18**) increased $^{AVG}K_{cis/trans}$ by two-fold, again commensurate with side chain steric bulk. In contrast, increasing the steric bulk at the *N*-β-carbon, as with *sb* (**19**) and *ipe* (**20**), did not have any significant effect on $^{AVG}K_{cis/trans}$, giving values similar to those observed for *ip* (**18**) and the cyclohexyl side chain (*ch*, **4**; Table 3). We also examined a (trimethylsilyl)methyl side chain (*tmsm*, **21**) as part of an effort to determine whether a lack of steric bulk at the *N*-α-position might be compensated for by an even larger increase in bulk at the *N*-β-position relative to the *ipe* side chain. Although the $K_{cis/trans}$ values for **21** were indeed higher than those of the aliphatic side chain model systems, analysis of this system is complicated by the possibility of dative oxygen-silicon bonding between the side chain silyl group and the acetamide oxygen. We suggest that this class of interactions could also be useful for controlling amide isomerism in peptoids, and is worthy of study in the future.

Turning our attention to the sterics of aromatic side chains, we appended a methyl group to the well-characterized *pe* side chain to determine if such modifications could be used to increase $K_{cis/trans}$ (*1pp*, **22**; Table 4). As expected, we observed a modest (20%) increase in $^{AVG}K_{cis/trans}$ relative to *pe* (**3**); this increase was nearly identical in each solvent tested, strongly suggesting a steric origin for the increase. Similar reasoning explains the lower $K_{cis/trans}$ values determined for the *N*-benzyl compounds *pm-Me* (**23**) and *pm-Pip* (**24**), as compared to the *pe-Me* (**6**) and *pe-Pip* (**3**) systems containing an *N*-α-methyl group (Table 2). Intriguingly, the absence of an *N*-α-methyl group in the side chain of *pm-Pip* (**24**), in conjunction with the presence of a piperidinyl amide at the C-terminus, especially promotes the *trans*-acetamide, since $K_{cis/trans}$ for *pm-Pip* (**24**) is dramatically lower (by 50%, on average) than that for *pm-Me* (**23**) in all solvents examined, while *pe-Me* (**6**) and *pe-Pip* (**3**) exhibit more similar $K_{cis/trans}$ values.

In an effort to more dramatically regulate amide isomerism using steric interactions, we constructed model systems containing naphthylethyl side chains (*2npe-Pip*, **25** and *1npe-Pip*, **26**; Table 4). We conjectured that the expanded size of these side chains could multiply steric interactions with nearby atoms, thereby restricting bond rotations. Furthermore, the electronic perturbation resulting from expansion of the aromatic ring system might simultaneously engender strong $n\rightarrow\pi^*_{Ar}$ interactions. Although the model system containing the 2-substituted naphthyl group (**25**) displayed only a slight increase in $K_{cis/trans}$ compared to the related aromatic side chain *pe* (in **3**), the 1-substituted naphthyl group (in **26**) largely suppressed the *trans*-acetamide rotamer. Preliminary molecular mechanics calculations suggest that steric interactions between the naphthyl side chain and the backbone of **26** restrict rotation of the naphthyl group such that $n\rightarrow\pi^*_{Ar}$ interactions

stabilizing the *cis*-rotamer are favored; these steric interactions are calculated to be significantly less severe in **25** (see Supporting Information.) The strong *cis*-rotameric preference elicited by the 1-naphthylethyl side chain, if representative of that within a polypeptoid, suggests that this side chain could prove exceptionally useful for the construction of peptoid helices. We return to this possibility below.

Investigations of the impact of hydrogen bonding interactions on peptoid amide rotamer equilibria

Hydrogen bonds are ubiquitous in peptide and protein structures, and are also essential to the folding of many non-natural foldamer classes.[21] Peptoids offer the distinctive opportunity to engineer the locations of all hydrogen bond donors *via* side chain selection, while conserving structural elements that promote folding. The strength of typical hydrogen bonds in organic solvents (up to 3 kcal/mol) relative to other noncovalent interactions makes them attractive architectural elements, and they have been exploited previously to stabilize peptoid structures (*e.g.*, the threaded loop, *vide supra*).[24, 28, 31] We therefore undertook a study of a set of peptoid model systems containing side chains capable of hydrogen bonding to the peptoid backbone (**27**–**32**; Figure 7).

We commenced our investigations of hydrogen bonding by examining the primary amide side chain *fipa* (**27**), derived from phenylalanine (Figure 7). We initially considered the possibility that a hydrogen bond could form between this side chain amide and the *N*-terminal acetamide, stabilizing the *cis*-acetamide isomer (Figure 8A), even though such γ-turn motifs are rare in peptides.[63] However, $K_{cis/trans}$ for **27** (Table 5) increased in the hydrogen bonding solvent methanol and decreased in the nonpolar solvent chloroform, implying that a side chain-acetamide hydrogen bond does not significantly affect the rotameric ratio of **27**. Furthermore, the downfield chemical shift of the amide side chain proton in the *trans*-acetamide relative to the *cis*-acetamide in the ^{1}H NMR spectrum of **27** (in acetonitrile and chloroform) suggests that any hydrogen bonds formed are stronger in the *trans*-acetamide than in the *cis*-acetamide (see Supporting Information).[64]

We reasoned that modulating the strength of the putative hydrogen bonds in the peptoid model systems might inform our understanding of how they affect $K_{cis/trans}$ in these systems. To this end, we examined additional model systems in which the secondary amide substituent on the side chain was systematically altered (**28**–**30;** Figure 7, Table 5). (We note that NMR spectroscopy did not detect any *trans*-rotamers (as defined in Table 2) of the side chain secondary amides of this series.) The $^{CD_3CN}K_{cis/trans}$ values obtained increased concomitantly with the expected acidity of the secondary amide proton; however, a direct hydrogen bond to the *cis*-acetamide seemed unlikely (Figure 8A; see discussion of **27** above). Based on these observations and NOESY data for **27** and **30**,[32] we hypothesized that a hydrogen bond preferentially forms between the side chain and the piperidinyl amide instead, leaving $K_{cis/trans}$ to be determined by the relative energies of competing backbone-side chain (Figure 8B; favoring *cis*) and backbone-backbone (Figure 8C; favoring *trans*) $n\rightarrow\pi^*_{C=O}$ interactions. Convincing solid state evidence for this hypothesis was provided by our previously reported X-ray crystal structure of the *fpnan* system (**30**), which exhibits both the hydrogen bond and the $n\rightarrow\pi^*_{C=O}$ interaction shown in Figure 8B.[32] The strong (≥10:1) preference for the *cis*-acetamide in acetonitrile, coupled with the NOESY data, also corroborates this model for stabilization of the *cis*-acetamide. As with the previously examined systems containing the *C*-terminal piperidinyl amide (*vide supra*), the $^{CD_3OD}K_{cis/trans}$ values for **27**–**29** and **30** were typically lower than the $^{CD_3CN}K_{cis/trans}$ values, while $^{CDCl_3}K_{cis/trans}$ values were uniformly low as compared to the other solvents examined, consistent with stronger backbone-backbone $n\rightarrow\pi^*_{C=O}$ interactions (Figure 8C) in this solvent. This solvent trend suggested that the tertiary piperidinyl amide, being more polarizable than the side chain secondary amide, might be more sensitive to solvent polarity

and could out-compete the side chain amide as the acceptor of the n →π *$_{C=O}$ interaction with the acetamide in chloroform; this solvent-dependent, divergent behavior of secondary and tertiary amides has been reported previously.[65]

In order to further evaluate this theory, we replaced the amide hydrogen bond donor in the side chain with an ester (**31**, Table 5), an excellent acceptor of n→π*$_{C=O}$ interactions (see above). As expected, ^{CD_3CN} $\Delta G_{cis/trans}$ significantly decreased (by 0.33 kcal/mol) versus amide **27**, confirming that any hydrogen bonding that occurs is not required for stabilizing the *cis*-acetamide, and further supporting our hypothesis that backbone-to-side chain n→π *$_{C=O}$ interactions (Figure 8B) stabilize the *cis*-acetamide rotamer in this series. Moreover, $\Delta G_{cis/trans}$ for **31** in chloroform also decreased by ~0.3 kcal/mol compared to **27**, signifying that this backbone-side chain n→π*$_{C=O}$ interaction is mostly unaffected by solvent polarity *per se*, again in line with expectations for the relatively non-polarizable ester (*vide supra*). However, $\Delta G_{cis/trans}$ values for amides **29** and **30** decreased by varying amounts in the hydrogen bonding solvent methanol relative to acetonitrile, and were generally *lower* than for ester **31**, even though esters are typically better acceptors of n→π*$_{C=O}$ interactions. These findings, in conjunction with the X-ray crystal structure of **30**, suggest that a hydrogen bond can stabilize a conformation (observed in the solid state) that predisposes the backbone and side chain amides to participate in an n→π*$_{C=O}$ interaction (Figure 8B). In this respect, the hydrogen bond appears to perform a similar function to that of the steric interactions in 1-naphthylethyl system **26**, in that it serves to enforce a conformational bias that engenders an n→π interaction. The significance of this hydrogen bond is underscored by the fact that a significant *decrease* of $\Delta G_{cis/trans}$ in methanol vs. acetonitrile is observed *only* for the compounds with amide side chains, which would be susceptible to hydrogen bond disruption by the solvent. (Note, solvent-mediated enhancement of backbone-backbone n→π*$_{C=O}$ interactions in methanol, such as that observed for **2**–**4** and **13**–**15** above, could also play a role in lowering $\Delta G_{cis/trans}$.) On the other hand, strengthening of the backbone-backbone n→π*$_{C=O}$ interactions (Figure 8C) due to reduced polarization of the piperidinyl amide in chloroform again appears to be the major factor contributing to the reduction of $K_{cis/trans}$ in chloroform versus acetonitrile for **28**–**30** (*vide supra*). Further confirmation of this finding was obtained by examining **32**, which lacked the piperidinyl amide cap and therefore exhibited uniformly higher (as compared to **31)** and nearly identical $K_{cis/trans}$ values for **32** in the three solvents examined, *including* chloroform. Indeed, the nearly identical $^{CD_3CN}\Delta G_{cis/trans}$ values for **31** and **32** indicate that backbone-backbone n→π *$_{C=O}$ interactions (Figure 8C) are virtually nonexistent in acetonitrile. These data also eliminate the possibility of significant n→π *$_{C=O}$ interactions between the backbone piperidinyl amide and the side chain ester.

Overall, the data acquired for this series of model systems (**27**–**32**) demonstrate that this class of side chain amide hydrogen bond donors does not directly interact with the *N*-terminal amide to dictate $K_{cis/trans}$ (Figure 8A). Rather, our results suggest that solvent-dependent hydrogen bonding and amide polarization affect the energies of the competing backbone-side chain (Figure 8B, favoring *cis*) and backbone-backbone (Figure 8C, favoring *trans*) n→π*$_{C=O}$ interactions that determine $K_{cis/trans}$. In light of the data above, incorporation of amide side chains into peptoids could constitute a highly effective strategy for promoting *cis*-amides in the peptoid backbone in polar solvents, as evidenced by the large *cis*/*trans* ratios exhibited by acetanilide **29** (~5:1), and especially **30** (≥10:1), in acetonitrile. Intriguingly, this same side chain class might also be used to construct new and optically active, *trans*-amide peptoid secondary structures in nonpolar solvents, since its capacity to stabilize *trans*-amides in chloroform rivals the other side chains in this report.[30] In general, the wide range of $K_{cis/trans}$ values attainable using side chain amides, coupled with their synthetic accessibility via standard coupling techniques, suggests that this side

chain class could be extremely useful for rationally tuning amide isomerism in the peptoid backbone.

Studies of Peptoid Oligomers Derived from the Model Systems

The peptoid model systems discussed above were designed to investigate interactions between peptoid side chains and the backbone, and thus typically consisted of a single side chain flanked by two backbone carbonyls. In a peptoid oligomer, however, each backbone carbonyl is in turn typically surrounded by two peptoid side chains, which may act cooperatively or competitively to influence amide rotameric equilibria. Therefore, peptoids containing at least two side chains could validate a role for the noncovalent interactions discussed above in directing amide isomerism within larger peptoid oligomers. To this end, we synthesized several polypeptoids (**33**–**38**, Figure 9) that were designed to probe these noncovalent interactions within peptoid oligomers, and analyzed their ^{1}H-COSY and HSQCAD NMR spectra in CD_3CN to determine backbone amide *cis*/*trans* ratios (Table 6).

At the outset, we were most interested in examining $n\rightarrow\pi^*_{Ar}$ interactions in polypeptoids, since these were expected to promote peptoid helix formation by stabilizing backbone *cis*-amides. We therefore incorporated a single *snp* residue (the *S*-enantiomer of the *np* side chain) within an *spe* pentamer at the central position away from the termini, in an attempt to minimize interference with its *cis*/*trans* ratio by hydrogen bonding to the *C*-terminus and to more accurately simulate the structural environment within longer peptoids. We were gratified to observe that this *snp* side chain, which exhibited a $K_{cis/trans}$ of ~3.3 in the methyl (**5**) and piperidinyl (**2**) model systems, significantly increased the population of *cis*-amides in **33** relative to the *spe* homopentamer **34** (Table 6). We subsequently examined two pentamers containing the *sfe* residue (**35** and **36**), which exhibited excellent resolution of signals by residue type in their HSQCAD spectra.[37] Once again, we found that our model systems were qualitatively predictive of $K_{cis/trans}$ in peptoid **35**, with the *sfe* residues exhibiting an even higher (46%) $^{CD_3CN}K_{cis/trans}$ value than the corresponding model system (**1**), and a six-fold higher $^{CD_3CN}K_{cis/trans}$ than the *spe* residues. Interestingly, the *overall cis*/*trans* ratios for the homopentamers **34** and **36** were found to be somewhat *lower* than those of the corresponding monomeric model systems. Since previous studies have demonstrated that hydrogen bonding at peptoid termini in related systems can profoundly affect conformation, especially by locally promoting *trans*-amides,[23, 25, 31, 37] we suggest that hydrogen bonding at the termini of these pentamers may have a similar impact.[66] This assertion is supported by the low $K_{cis/trans}$ values obtained for the *spe* residues of the mixed oligomer **35**, two of which constitute the terminal residues. Notwithstanding such hydrogen bonding-derived effects, these findings demonstrate that $n\rightarrow\pi^*_{Ar}$ interactions can indeed regulate amide isomerism at internal residues of *N*-α-chiral aromatic polypeptoids, and can be used to rationally control peptoid structure.

We next constructed homooligomers composed of (*S*)-1-naphthylethyl (*s1npe*) side chains (**37** and **38**, Table 6), since the consistently high $K_{cis/trans}$ values obtained using this side chain suggested that it could prove particularly useful for constructing robust peptoid helices. We were pleased to observe that the very high $K_{cis/trans}$ observed for the monomeric system (**26**; 6.27) in acetonitrile was amplified in the *s1npe* homooligomers in a length-dependent manner, delivering a $^{CD_3?CN}K_{cis/trans}$ of 7.0 and 9.7 in the dimer (**37**) and trimer (**38**), respectively – to our knowledge, the highest overall amide *cis*/*trans* ratios observed for any acyclic peptoid oligomers to date. This length-dependent amplification of $K_{cis/trans}$ is indicative of cooperatively stabilized structure — a hallmark of well-folded peptoids — although the nature of such cooperative effects has not been examined extensively so far.[23, 67]

To gain additional insight into the structures of **37** and **38**, we obtained their circular dichroism (CD) spectra in acetonitrile. The CD spectra of **37**, and of **38** in particular, contained very intense extrema (Figure 10), especially near 220 nm, which has been associated with the presence of *cis*-amides[23, 31] and helical peptoids in general.[25, 31] Comparison of these spectra with those of the corresponding optically active model system (*S*-**26**) reveals a striking length-dependent increase in ellipticity per amide, again suggestive of a cooperatively folded secondary structure.[29] In conjunction with the NMR data, these findings establish that *1npe* is highly effective for inducing local *cis*-amide conformations in polypeptoids. Moreover, a reduction in the number of correlations in the HSQCAD NMR (see Supporting Information) and concomitant increase in CD signal strength data with increasing oligomer length, as observed in these systems, have been cited as evidence for increasing conformational homogeneity as a function of oligomer length.[26] Given that *spe* pentamer **34** has been shown to be more structured than the analogous *spe* trimer,[23] the significantly higher (more than 6-fold) overall $K_{cis/trans}$ measured for *1npe* trimer **38** as compared to *spe* pentamer **34** (Table 6) suggests that incorporation of *1npe* may permit the construction of extremely robust peptoid helices. Indeed, the intensity of the CD signal at 220 nm for trimer **38** is more than twice that reported for pentamer **34**[37] and its enantiomer.[23] In light of these data, a much higher degree of side chain diversity than was previously possible in designed peptoid helices may be achievable by using the *1npe* side chain to reduce the number of residues dedicated to maintaining structural integrity.[22]

Summary

This comprehensive study has revealed several new strategies for controlling peptoid amide isomerism using noncovalent interactions, including n→π*, steric, and hydrogen bonding interactions. These strategies were developed through the design, synthesis, and characterization of small, model peptoid systems, which were shown to be largely predictive of the rotameric equilibria of the backbone amides in *N*-α-chiral aromatic peptoid oligomers, an important and often utilized class of peptoids. One of the most significant findings of this study is that *cis*-amides in the peptoid backbone can be *exclusively* promoted by select *N*-α-chiral acetanilide and *N*-1-naphthylethyl side chains, putatively by n →π $*_{C=O}$/hydrogen bonding interactions and n→π $*_{Ar}$/steric interactions, respectively. In the former case, the relative polarizabilities of the side chain- versus backbone-amides appear to give rise to the dramatic solvent effects observed, with nonpolar solvents reversing the *cis*-amide preference in the peptoid backbone. This phenomenon evokes an intriguing new possibility for peptoid structural design entailing the rational tuning of backbone- and side chain-amide electronics to stabilize either *cis*- or *trans*-amides, potentially generating novel peptoid structures that can also fold in a solvent-dependent manner.[28] The subtle and solvent-dependent interplay of n→π*, steric, and hydrogen bonding interactions in peptoids has not been previously investigated; these findings could thus provide a framework for further development of new peptoid design strategies.

The application of one of the new design tactics reported herein – the incorporation of *N*-1-naphthylethyl side chains into peptoids – yielded peptoid oligomers that exhibited unprecedented conformational homogeneity. In this context, the structure-promoting elements presented here should prove especially useful for constructing well-folded peptoid scaffolds with an expanded number of side chain sites available for rational or combinatorial diversification. In addition to elucidating aspects of the regulation of peptoid amide isomerism *via* noncovalent interactions, these findings may also be useful in other foldamer regimes employing tertiary amides. As a whole, this work significantly expands the available repertoire of peptoid design strategies, and should enable the construction of both familiar and as of yet uncharacterized peptoid architectures.

Supplementary Material

Refer to Web version on PubMed Central for supplementary material.

Acknowledgments

We thank the NSF (CHE-0449959), ONR (N000140710255), Burroughs Wellcome Fund, Research Corporation, Dreyfus Foundation, Johnson & Johnson, and 3M for financial support of this work. H.E.B is an Alfred P. Sloan Foundation fellow. S.A.F. acknowledges the ACS Division of Medicinal Chemistry for a pre-doctoral fellowship (sponsored by Sanofi-Aventis) and Pfizer Global R&D for a Diversity in Organic Chemistry Fellowship. Support for the NMR facilities at UW-Madison by the NIH (1 S10 RR13866-01 and 1 S10 RR08389-01) and the NSF (CHE-0342998 and CHE-9629688) is gratefully acknowledged. We thank Professors Ronald Raines and Samuel Gellman for many contributive discussions, and Dr. Grant Geske for computational experiments.

References and Notes

1. Simon RJ, et al. Proc Natl Acad Sci U S A. 1992; 89:9367–9371. [PubMed: 1409642]
2. Figliozzi GM, Goldsmith R, Ng SC, Banville SC, Zuckermann RN. Methods Enzymol. 1996; 267:437–447. [PubMed: 8743331]
3. Zuckermann RN, Kerr JM, Kent SBH, Moos WH. J Am Chem Soc. 1992; 114:10646–10647.
4. Miller SM, Simon RJ, Ng S, Zuckermann RN, Kerr JM, Moos WH. Bioorg Med Chem Lett. 1994; 4:2657–2662.
5. Kwon YU, Kodadek T. J Am Chem Soc. 2007; 129:1508–1509. [PubMed: 17283989]
6. Patch JA, Barron AE. J Am Chem Soc. 2003; 125:12092–12093. [PubMed: 14518985]
7. Mora P, Masip I, Cortes N, Marquina R, Merino R, Merino J, Carbonell T, Mingarro I, Messeguer A, Perez-Paya E. J Med Chem. 2005; 48:1265–1268. [PubMed: 15715495]
8. Wu CW, Seurynck SL, Lee KYC, Barron AE. Chem Biol. 2003; 10:1057–1063. [PubMed: 14652073]
9. Wender PA, Mitchell DJ, Pattabiraman K, Pelkey ET, Steinman L, Rothbard JB. Proc Natl Acad Sci U S A. 2000; 97:13003–13008. [PubMed: 11087855]
10. Hara T, Durell SR, Myers MC, Appella DH. J Am Chem Soc. 2006; 128:1995–2004. [PubMed: 16464101]
11. Zuckermann RN, Martin EJ, Spellmeyer DC, Stauber GB, Shoemaker KR, Kerr JM, Figliozzi GM, Goff DA, Siani MA, Simon RJ. J Med Chem. 1994; 37:2678–2685. [PubMed: 8064796]
12. Nguyen JT, Porter M, Amoui M, Miller WT, Zuckermann RN, Lim WA. Chem Biol. 2000; 7:463–473. [PubMed: 10903934]
13. Haynes RD, Meagher RJ, Won JI, Bogdan FM, Barron AE. Bioconjugate Chem. 2005; 16:929–938.
14. Reddy MM, Kodadek T. Proc Natl Acad Sci U S A. 2005; 102:12672–12677. [PubMed: 16123137]
15. Pirrung MC, Park K, Tumey LN. J Comb Chem. 2002; 4:329–344. [PubMed: 12099851]
16. Maayan G, Ward MD, Kirshenbaum K. Proc Natl Acad Sci U S A. 2009; 106:13679–13684. [PubMed: 19667204]
17. Houghten RA, Pinilla C, Giulianotti MA, Appel JR, Dooley CT, Nefzi A, Ostresh JM, Yu Y, Maggiora GM, Medina-Franco JL, Brunner D, Schneider J. J Comb Chem. 2008; 10:3–19. [PubMed: 18067268]
18. Le GT, Abbenante G, Becker B, Grathwohl M, Halliday J, Tometzki G, Zuegg J, Meutermans W. Drug Discov Today. 2003; 8:701–709. [PubMed: 12927513]
19. Trabocchi A, Menchi G, Guarna F, Machetti F, Scarpi D, Guarna A. Synlett. 2006:331–353.
20. Herman RE, Badders D, Fuller M, Makienko EG, Houston ME Jr, Quay SC, Johnson PH. J Biol Chem. 2007; 282:9813–9824. [PubMed: 17264074]
21. Gellman SH. Acc Chem Res. 1998; 31:173–180.
22. Wu CW, Sanborn TJ, Huang K, Zuckermann RN, Barron AE. J Am Chem Soc. 2001; 123:6778–6784. [PubMed: 11448181]

23. Wu CW, Sanborn TJ, Zuckermann RN, Barron AE. J Am Chem Soc. 2001; 123:2958–2963. [PubMed: 11457005]
24. Sanborn TJ, Wu CW, Zuckermann RN, Barron AE. Biopolymers. 2002; 63:12–20. [PubMed: 11754344]
25. Armand P, Kirshenbaum K, Goldsmith RA, Farr-Jones S, Barron AE, Truong KT, Dill KA, Mierke DF, Cohen FE, Zuckermann RN, Bradley EK. Proc Natl Acad Sci U S A. 1998; 95:4309–4314. [PubMed: 9539733]
26. Wu CW, Kirshenbaum K, Sanborn TJ, Patch JA, Huang K, Dill KA, Zuckermann RN, Barron AE. J Am Chem Soc. 2003; 125:13525–13530. [PubMed: 14583049]
27. Armand P, Kirshenbaum K, Falicov A, Dunbrack RL Jr, Dill KA, Zuckermann RN, Cohen FE. Fold Des. 1997; 2:369–375. [PubMed: 9427011]
28. Shin SBY, Kirshenbaum K. Org Lett. 2007; 9:5003–5006. [PubMed: 17960939]
29. Kirshenbaum K, Barron AE, Goldsmith RA, Armand P, Bradley EK, Truong KT, Dill KA, Cohen FE, Zuckermann RN. Proc Natl Acad Sci U S A. 1998; 95:4303–4308. [PubMed: 9539732]
30. Shah NH, Butterfoss GL, Nguyen K, Yoo B, Bonneau R, Rabenstein DL, Kirshenbaum K. J Am Chem Soc. 2008; 130:16622–16632. [PubMed: 19049458]
31. Huang K, Wu CW, Sanborn TJ, Patch JA, Kirshenbaum K, Zuckermann RN, Barron AE, Radhakrishnan I. J Am Chem Soc. 2006; 128:1733–1738. [PubMed: 16448149]
32. Gorske BC, Bastian BL, Geske GD, Blackwell HE. J Am Chem Soc. 2007; 129:8928–8929. [PubMed: 17608423]
33. Hodges JA, Raines RT. Org Lett. 2006; 8:4695–4697. [PubMed: 17020280]
34. Still WC, Kahn M, Mitra A. J Org Chem. 1978; 43:2923–2925.
35. Goddard, TD.; Kneller, DG. SPARKY, v. 3.110. University of California; San Francisco:
36. Gorske BC, Jewell SA, Guerard EJ, Blackwell HE. Org Lett. 2005; 7:1521–1524. [PubMed: 15816742]
37. Gorske BC, Blackwell HE. J Am Chem Soc. 2006; 128:14378–14387. [PubMed: 17076512]
38. Boyer RD, Johnson R, Krishnamurthy K. J Magn Reson. 2003; 165:253–259. [PubMed: 14643707]
39. Fowler SA, Luechapanichkul R, Blackwell HE. J Org Chem. 2009; 74:1440–1449. [PubMed: 19159244]
40. Toth G, Koever KE, Murphy RF, Lovas S. J Phys Chem B. 2004; 108:9287–9296.
41. Gamez P, Mooibroek TJ, Teat SJ, Reedijk J. Acc Chem Res. 2007; 40:435–444. [PubMed: 17439191]
42. Egli M, Sarkhel S. Acc Chem Res. 2007; 40:197–205. [PubMed: 17370991]
43. Qian X, Xu X, Li Z, Frontera A. Chem Phys Lett. 2003; 372:489–496.
44. Madison V, Kopple KD. J Am Chem Soc. 1980; 102:4855–4863.
45. Cubberley MS, Iverson BL. J Am Chem Soc. 2001; 123:7560–7563. [PubMed: 11480976]
46. Hill DJ, Moore JS. Proc Natl Acad Sci U S A. 2002; 99:5053–5057. [PubMed: 11917139]
47. Hinderaker MP, Raines RT. Protein Sci. 2003; 12:1188–1194. [PubMed: 12761389]
48. Bretscher LE, Jenkins CL, Taylor KM, DeRider ML, Raines RT. J Am Chem Soc. 2001; 123:777–778. [PubMed: 11456609]
49. Hodges JA, Raines RT. J Am Chem Soc. 2003; 125:9262–9263. [PubMed: 12889933]
50. Kumin M, Sonntag LS, Wennemers H. J Am Chem Soc. 2007; 129:466–467. [PubMed: 17226990]
51. Neuvonen H, Neuvonen K, Koch A, Kleinpeter E, Pasanen P. J Org Chem. 2002; 67:6995–7003. [PubMed: 12353992]
52. Bromilow J, Brownlee RTC, Craik DJ, Fiske PR, Rowe JE, Sadek M. J Chem Soc, Perkin Trans. 1981; 2:753–759.
53. DeRider ML, Wilkens SJ, Waddell MJ, Bretscher LE, Weinhold F, Raines RT, Markley JL. J Am Chem Soc. 2002; 124:2497–2505. [PubMed: 11890798]
54. Choudhary A, Gandla D, Krow GR, Raines RT. J Am Chem Soc. 2009; 131:7244–7246. [PubMed: 19469574]
55. Wiberg KB, Laidig KE. J Am Chem Soc. 2002; 109:5935–5943.

56. Wiberg, KB. Origin of the Amide Rotational Barrier. In: Greenberg, A.; Breneman, CM.; Liebman, JF., editors. The Amide Linkage: Structural Significance in Chemistry, Biochemistry, and Materials Science. Wiley-IEEE; New York: 2002. p. 33-46.
57. Eberhardt ES, Loh SN, Hinck AP, Raines RT. J Am Chem Soc. 1992; 114:5437–5439. [PubMed: 21451730]
58. Nakanishi H, Fujita H, Yamamoto O. Bull Chem Soc Jpn. 1978; 51:214–218.
59. Cox C, Lectka T. J Org Chem. 1998; 63:2426–2427. [PubMed: 11672097]
60. Kemnitz CR, Loewen MJ. J Am Chem Soc. 2007; 129:2521–2528. [PubMed: 17295481]
61. Gordy W, Stanford SC. J Chem Phys. 1941; 9:204–214.
62. Stewart WE, Siddall TH. Chem Rev. 1970; 70:517–551.
63. Yang D, Li W, Qu J, Luo SW, Wu YD. J Am Chem Soc. 2003; 125:13018–13019. [PubMed: 14570462] and references therein
64. Wagner G, Pardi A, Wuethrich K. J Am Chem Soc. 1983; 105:5948–5949.
65. Jordan T, Mukerji I, Wang Y, Spiro TG. J Mol Struct. 1996; 379:51–64.
66. We note that the ammonium groups at the *N*-termini of the analogous, unacylated peptoids (see reference 37) would also be expected to form strong hydrogen bonds that could account for the similar overall $K_{cis/trans}$ values observed for these systems.
67. Lee BC, Zuckermann RN, Dill KA. J Am Chem Soc. 2005; 127:10999–11009. [PubMed: 16076207]

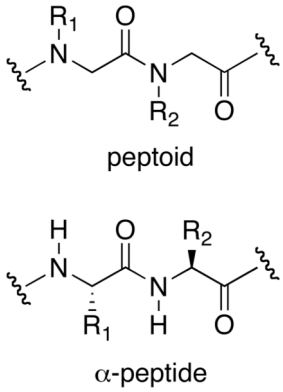

Figure 1.
Comparison of the peptoid and α-peptide primary structures.

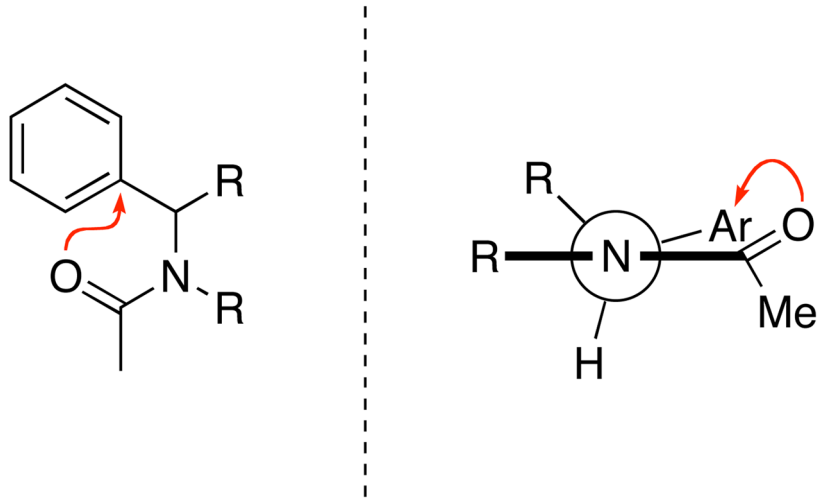

Figure 2.
Left: The n→π*$_{Ar}$ interaction (indicated by the red arrow) proposed to increase $K_{cis/trans}$ for peptoid backbone amides. *Right:* Newman projection depicting the n→π*$_{Ar}$ interaction.

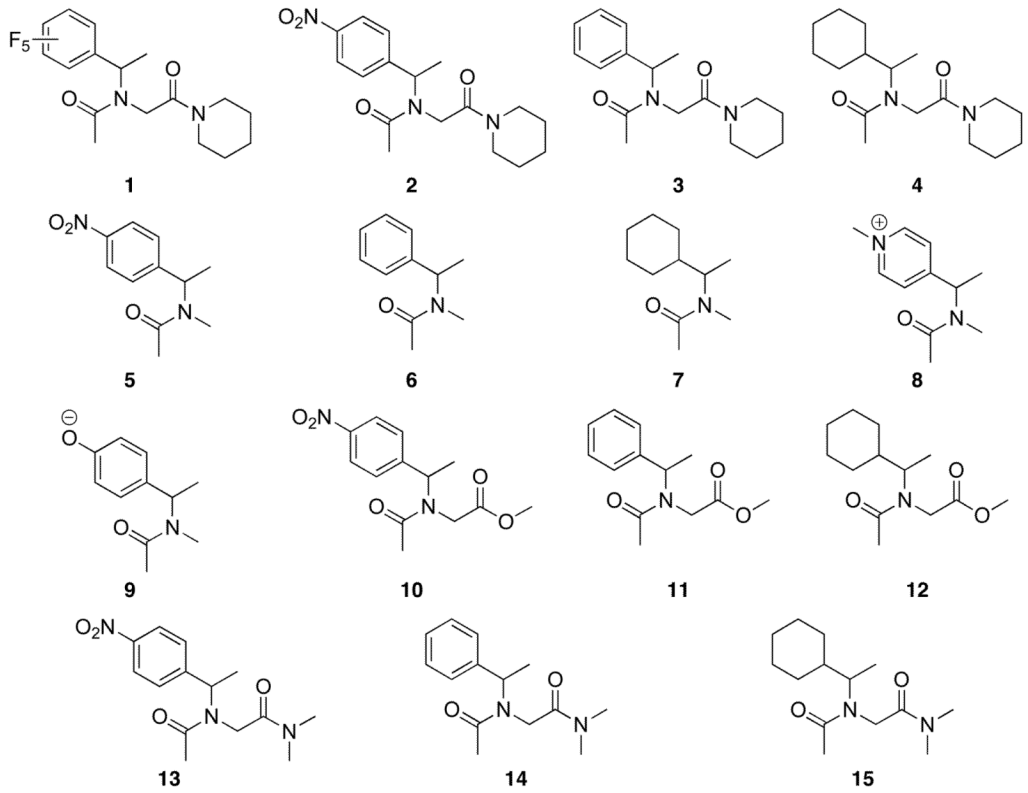

Figure 3.
Structures of the peptoid model systems (**1**–**15**) designed to probe n→π* interactions.

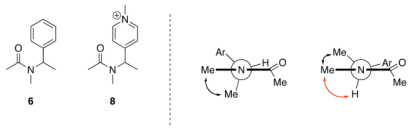

Figure 4.
Left: Structures of model compounds **6** and **8**. *Right:* Newman projections depicting the most populated conformations for *cis*-**6** and *cis*-**8**, as indicated by the NOEs shown: red=stronger for **8** v. **6**, black=identical for **6** and **8**.

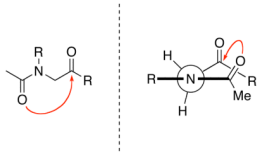

Figure 5.
Left: The n→π*$_{C=O}$ interaction (indicated by the red arrow) proposed to reduce $K_{cis/trans}$ for the donating amide in peptoids. *Right:* Newman projection depicting the n→π*$_{C=O}$ interaction

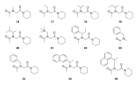

Figure 6.
Structures of the peptoid model systems (**16**–**26**) designed to probe steric interactions.

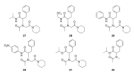

Figure 7.
Structures of the peptoid model systems (**27**–**32)** designed to probe hydrogen bonding interactions.

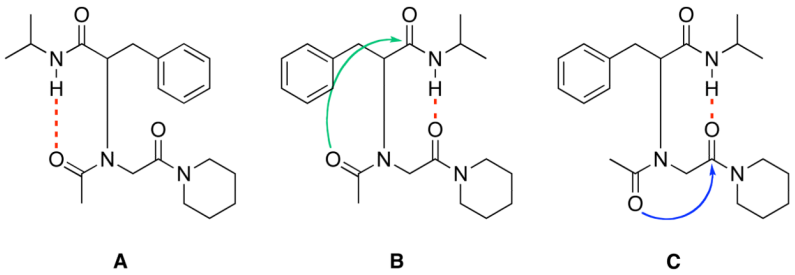

Figure 8.
Possible noncovalent interactions affecting $K_{cis/trans}$ for **27**. A) Direct hydrogen bond (red dashes) stabilizing the *cis*-acetamide. B) Backbone-side chain n→π*$_{C=O}$ interaction (green arrow) stabilizing the *cis*-acetamide. C) Backbone-backbone n→π*$_{C=O}$ interaction (blue arrow) stabilizing the *trans*-acetamide.

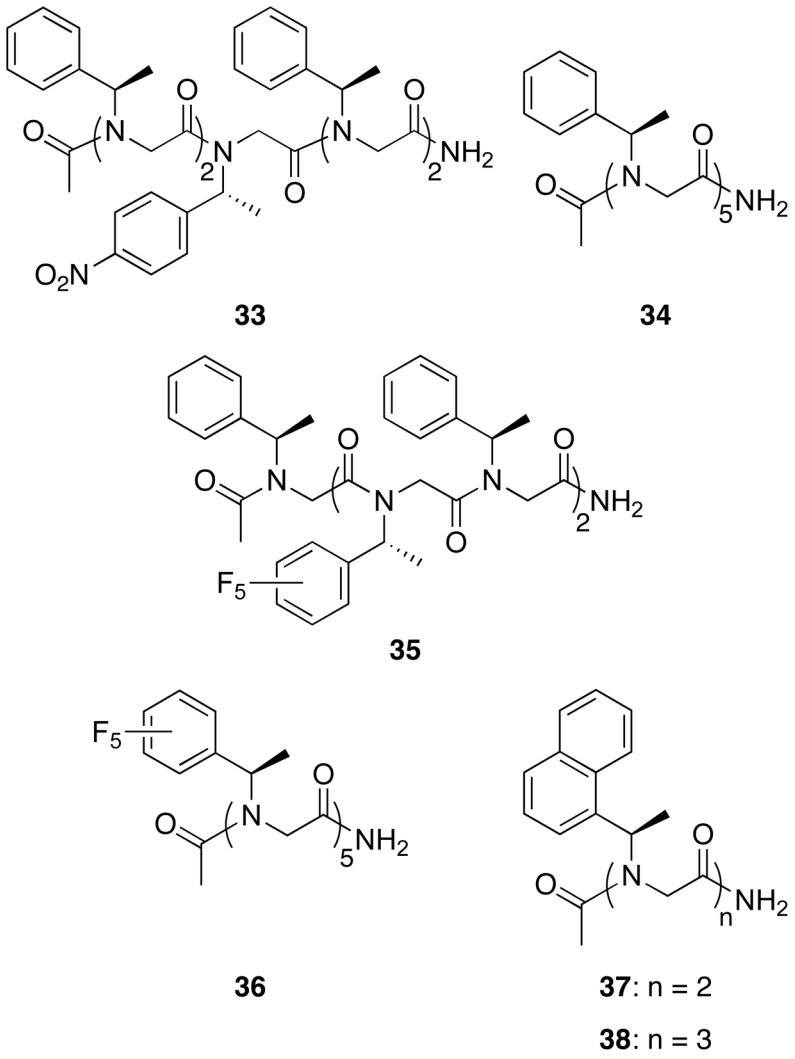

Figure 9.
Structures of the polypeptoids (**33**–**37)** designed to examine noncovalent interactions in peptoid oligomers.

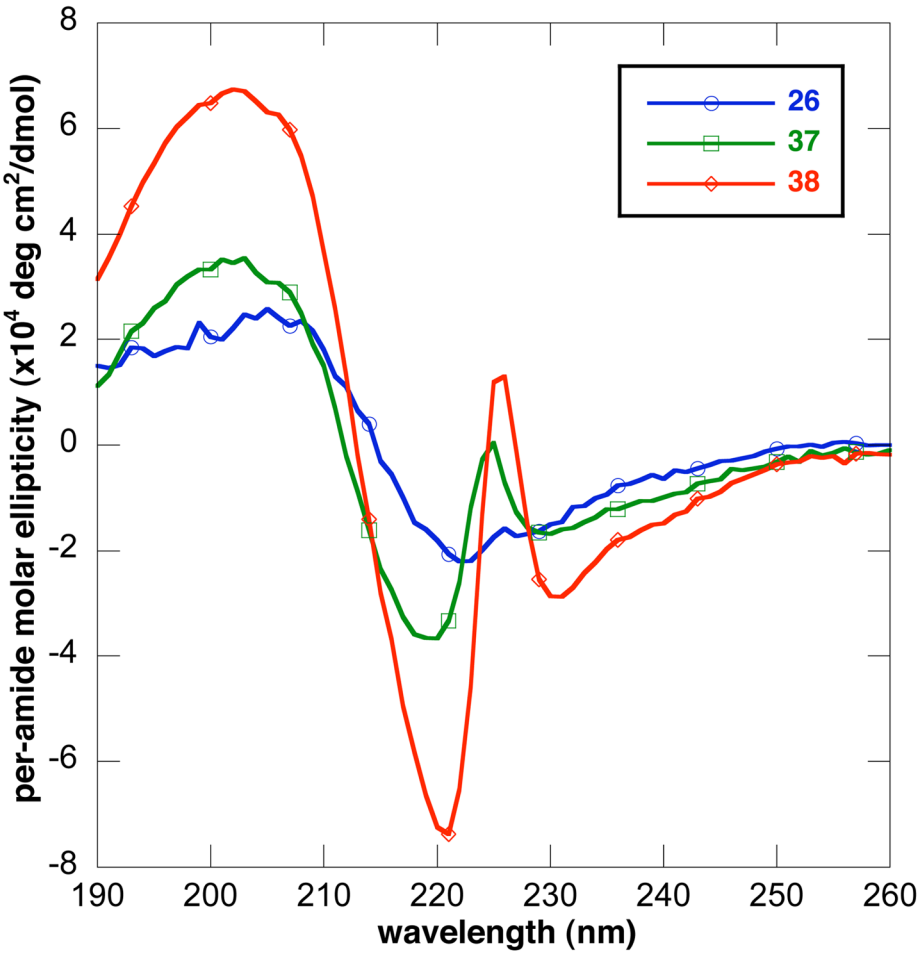

Figure 10.
CD spectra of Ac-*s1npe-Pip* (*S*-**26**), Ac-(*s1npe*)$_2$-CONH$_2$ (**37**), and Ac-(*s1npe*)$_3$-CONH$_2$ (**38**) at 60 μM concentration in acetonitrile. Spectra were collected at 25 °C.

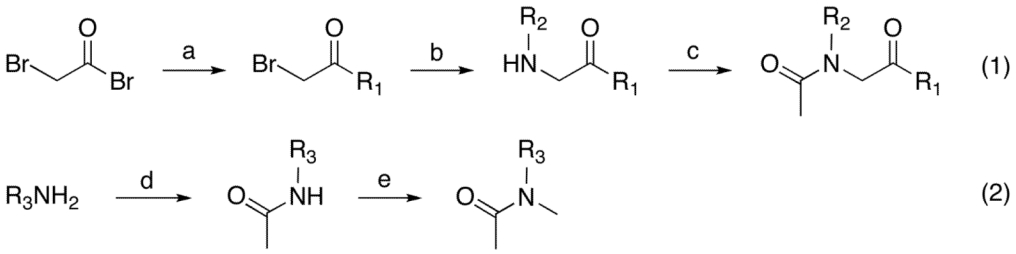

Scheme 1.

The generic synthetic routes (eqs 1 and 2) used in the construction of the peptoid model systems. Reagents and conditions: a. 0.9 equiv. R^1NH_2, 1 equiv. triethylamine, CH_2Cl_2, 0 °C, 60 min. b. 0.85 equiv. R^2NH_2, DMF, 0–24 °C, 12 h. c. 4 equiv. $(CH_3CO)_2O$, 2.1 equiv. $(i\text{-Pr})_2EtN$, CH_2Cl_2, 25 °C, 30 min. d. 2.1 equiv. $(CH_3CO)_2O$, CH_2Cl_2, 25 °C, 30 min. e. 2 equiv. NaH, 1.2 equiv. CH_3I, DMF, 0 °C, 5 min. Details of representative syntheses of these compound classes have been reported previously.[32]

Table 1

Structures, purities, and calculated and observed masses for peptoid pentamers **33**–**38**.

peptoid pentamer	monomer sequence (amino to carboxy terminus)[a]	% purity[b]	calculated mass	observed mass[c]
33	Ac-(*spe*)$_2$-*snp*-(*spe*)$_2$-CONH$_2$	95	909.4	932.1 [M+Na$^+$]$^+$
34	Ac-(*spe*)$_5$-CONH$_2$	99	864.5	887.1 [M+Na$^+$]$^+$
35	Ac-(*sfe*-*spe*)$_2$-*spe*-CONH$_2$	99	1044.4	1067.1 [M+Na$^+$]$^+$
36	Ac-(*sfe*)$_5$-CONH$_2$	99	1314.2	1337.1 [M+Na$^+$]$^+$
37	Ac-(*s1npe*)$_2$-CONH$_2$	99	481.2	504.1[M+Na$^+$]$^+$
38	Ac-(*s1npe*)$_3$-CONH$_2$	98	692.3	715.4 [M+Na$^+$]$^+$

[a] See text for definitions of peptoid monomer abbreviations.

[b] Determined by integration of the HPLC trace with UV detection at 220 nm.

[c] Mass spectrometry data were acquired using either ESI or MALDI-TOF techniques.

Table 2

Structure of the generic peptoid model system (top), and the structures and abbreviated names of the *C*-termini (R_1) and side chains (R_2) examined in this study.[a]

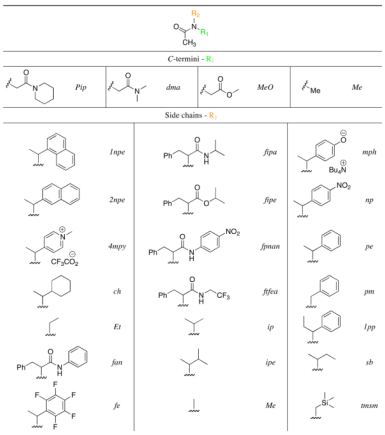

[a] Single stereocenters do not influence $K_{cis/trans}$ in these systems; enantiomeric excesses were therefore not determined. The *cis*-rotamer was defined as that which orients the side chain and the oxygen atom on the same side of the amide bond.

Table 3

Peptoid model system structures **1**–**15**, *N*-terminal acetamide *cis*/*trans* ratios in various solvents ($K_{cis/trans}$),[a] and corresponding free energy differences ($\Delta G_{cis/trans}$).[b] Standard deviations (SD) for $K_{cis/trans}$ were typically <10%.

			CD_3OD		CD_3CN		$CDCl_3$		C_6D_6		
entry	**R_1**	**R_2**	**$K_{cis/trans}$**	**ΔG (kcal/mol)**	**$K_{cis/trans}$**	**ΔG (kcal/mol)**	**$K_{cis/trans}$**	**ΔG (kcal/mol)**	**$K_{cis/trans}$**	**ΔG (kcal/mol)**	**$^{AVG}K_{cis/trans}$**
1	*Pip*	*fe*	2.46	−0.53	3.84	−0.79	1.60	−0.28	2.07	−0.43	2.49
2	*Pip*	*np*	1.84	−0.36	3.43	−0.73	1.53	−0.25	1.59	−0.28	2.10
3	*Pip*	*pe*	1.26	−0.14	2.04	−0.42	0.70	0.21	1.03	−0.02	1.26
4	*Pip*	*ch*	0.72	0.20	1.22	−0.12	0.31	0.69	0.37	0.59	0.66
5	*Me*	*np*	2.83	−0.61	3.27	−0.70	4.20	−0.85	4.31	−0.86	3.65
6	*Me*	*pe*	1.95	−0.40	2.12	−0.44	1.78	−0.34	2.46	−0.53	2.08
7	*Me*	*ch*	1.23	−0.12	1.30	−0.15	1.00	0.00	1.34	−0.18	1.22
8	*Me*	*4mpy*	6.79	−1.31	7.82	−1.22	>10	<−1.36	-- *c*	--	>8.20
9	*Me*	*mph*	1.82	−0.35	1.25	−0.13	1.69	−0.31	--	--	1.59
10	*MeO*	*np*	1.07	−0.04	1.05	−0.03	1.34	−0.17	1.20	−0.11	1.17
11	*MeO*	*pe*	0.75	0.17	0.67	0.24	0.66	0.25	0.68	0.22	0.69
12	*MeO*	*ch*	0.38	0.58	0.29	0.73	0.31	0.70	0.32	0.67	0.33
13	*dma*	*np*	1.54	−0.25	3.06	−0.66	1.12	−0.07	1.20	−0.11	1.73
14	*dma*	*pe*	1.13	−0.07	1.69	−0.31	0.54	0.36	0.70	0.21	1.02
15	*dma*	*ch*	0.71	0.20	0.58	0.33	0.25	0.82	0.42	0.52	0.49

[a] Determined by integrating ^{1}H NMR spectra of 15 mM solutions at 24 °C.

[b] $\Delta G = -RT\ln(K_{cis/trans})$.

[c] Data not available.

Table 4

Peptoid model system structures **16**–**26**, *N*-terminal acetamide *cis*/*trans* ratios in various solvents ($K_{cis/trans}$),[a] and corresponding free energy differences ($\Delta G_{cis/trans}$).[b] Solvents are listed in order of decreasing polarity. Standard deviations (SD) for $K_{cis/trans}$ did not exceed 10%.

			CD_3OD		CD_3CN		$CDCl_3$		C_6D_6		
entry	**R_1**	**R_2**	**$K_{cis/trans}$**	**ΔG (kcal/mol)**	**$K_{cis/trans}$**	**ΔG (kcal/mol)**	**$K_{cis/trans}$**	**ΔG (kcal/mol)**	**$K_{cis/trans}$**	**ΔG (kcal/mol)**	**$^{AVG}K_{cis/trans}$**
16	*Pip*	*Me*	0.42	0.52	0.60	0.30	0.15	1.10	0.17	1.04	0.34
17	*Pip*	*Et*	0.47	0.45	0.66	0.25	0.17	1.05	0.20	0.95	0.38
18	*Pip*	*ip*	0.64	0.26	1.09	−0.05	0.40	0.54	0.47	0.44	0.65
19	*Pip*	*sb*	0.64	0.26	1.05	−0.03	0.33	0.66	0.48	0.43	0.63
20	*Pip*	*ipe*	0.67	0.23	1.18	−0.10	0.33	0.65	0.48	0.43	0.67
21	*Pip*	*tmsm*	1.61	−0.28	1.91	−0.38	0.48	0.44	0.78	0.14	1.20
22	*Pip*	*1pp*	1.67	−0.30	2.20	−0.47	0.90	0.06	1.23	−0.12	1.50
23	*Me*	*pm*	1.49	−0.24	1.68	−0.31	1.30	−0.15	-- [c]	-- [c]	-- [c]
24	*Pip*	*pm*	0.62	0.28	1.15	−0.09	0.24	0.84	0.25	0.82	0.57
25	*Pip*	*2npe*	1.55	−0.26	2.21	−0.47	0.86	0.09	1.20	−0.11	1.46
26	*Pip*	*1npe*	4.63	−0.72	6.27	−1.08	2.60	−0.56	4.07	−0.83	4.39

[a] Determined by integrating ^{1}H NMR spectra of 15 mM solutions at 24 °C.

[b] $\Delta G = -RT\ln(K_{cis/trans})$.

[c] Data not available.

Table 5

Peptoid model system structures **27–32**, *N*-terminal acetamide *cis*/*trans* ratios in various solvents ($K_{cis/trans}$),[a] and corresponding free energy differences ($\Delta G_{cis/trans}$).[b] Solvents are listed in order of decreasing polarity. Standard deviations (SD) for $K_{cis/trans}$ did not exceed 10%, except for **30** in CD_3CN (SD = 20%).

			CD_3OD		CD_3CN		$CDCl_3$	
entry	**R_1**	**R_2**	**$K_{cis/trans}$**	**ΔG (kcal/mol)**	**$K_{cis/trans}$**	**ΔG (kcal/mol)**	**$K_{cis/trans}$**	**ΔG (kcal/mol)**
27	*Pip*	*fipa*	1.80	−0.35	1.56	−0.26	0.51	0.40
28	*Pip*	*ftfea*	2.77	−0.60	3.26	−0.70	0.86	0.09
29	*Pip*	*fan*	3.33	−0.71	4.57	−0.9	0.58	0.32
30	*Pip*	*fpnan*	-- [c]	--	≥10	≤ −1.36	--	--
31	*Pip*	*fipe*	1.39	−0.19	2.73	−0.59	0.82	0.12
32	*Me*	*fipe*	2.44	−0.53	2.58	−0.56	2.57	−0.56

[a] Determined by integrating ^{1}H NMR spectra of 15 mM solutions at 24 °C.

[b] $\Delta G = -RT\ln(K_{cis/trans})$.

[c] Data not available.

Table 6

Polypeptoid structures **33–38** and $K_{cis/trans}$ values for each residue type, as determined by ^{1}H-COSY and HSQCAD NMR in CD_3CN at 24°C.

entry	structure	*spe* $K_{cis/trans}$	*snp* $K_{cis/trans}$	*sfe* $K_{cis/trans}$	*s1npe* $K_{cis/trans}$	overall[b] $K_{cis/trans}$
33	Ac-(*spe*)$_2$-*snp*-(*spe*)$_2$-CONH$_2$	-- [a]	--			2.1
34	Ac-(*spe*)$_5$-CONH$_2$	1.5				1.5
35	Ac-(*sfe*-*spe*)$_2$-*spe*-CONH$_2$	0.9		5.6		1.7
36	Ac-(*sfe*)$_5$-CONH$_2$			2.8		2.8
37	Ac-(*s1npe*)$_2$-CONH$_2$				7.0	7.0
38	Ac-(*s1npe*)$_3$-CONH$_2$				9.7	9.7

[a] Data not available.

[b] Weighted average of $K_{cis/trans}$ for all residues.